PULLED MICROCAPILLARY TUBE RESONATORS FOR HIGH PRECISION MICRODROPLET SIZE MEASUREMENTS

Donghyuk Lee[1], Sangken. Kauh[1], and Jungchul Lee[2]
[1]Seoul National University, Seoul, KOREA
[2]Sogang University, Seoul, KOREA

ABSTRACT

This paper reports the high-precision microdroplet size measurement using a pulled microcapillary tube resonator (PμTR) which is fabricated by a microfabrication-free approach-pulling a glass capillary and fixing it on top of a machined jig. The pulled section in the middle makes simple contact with a piezoactuator (actuation node) and a quartz tuning fork (QTF, sensing node) while un-pulled sections at both ends provide easy connection with standard adapters and fluidic tubings. We introduce microscale oil droplets into the PμTR and demonstrate that the PμTR exhibits the resolution of 31 nm for the radius change of oil droplets at around the average radius of 28.47 μm. This resolution is far superior to the diffraction limit of conventional optical microscopy based techniques.

INTRODUCTION

Hollow resonators [1-4] have become one of the most promising platforms for inertial sensing of liquids and particle suspensions with the hollow core intrinsically serving as sample delivery and transport channel. The embedded channel localizes liquid samples and makes suspended particles guided toward the mass sensing region on demand. This is a unique advantage of hollow resonators over solid ones that are fully exposed to liquid sample and passively observe stochastic landing of suspended particles. Most hollow resonators reported to date have been made via sacrificial processes [1, 2] and fusion bonding [3, 4]. Hollow resonators have shown numerous applications with unprecedented performance such as mass, density, volume, and surface charge measurements of single micro-/nanoparticles and cells.

A novel approach by atomic migration of silicon recently reported has significantly simplified and expedited the overall fabrication of hollow resonators [5]. Nevertheless, this simple process still requires microfabrication facilities so that researchers who have no or limited access to them hardly take advantage of this technique. Interestingly, a commercially available microcapillary suspended over a pre-defined trench seems very promising since it is potentially available to anyone. Suspended microcapillary resonators with optical detection were employed for liquid density measurements [6] and differentiation of X- and Y- chromosome bearing sperm cells [7]. However, optical detection makes the overall system bulky and requires a precise alignment. In addition, small inner and outer diameters of microcapillaries are not directly compatible with existing standard fluidic tubings and connectors.

Here, we introduce an innovative solution for aforementioned issues—a hollow microchannel mass sensing system which exhibits user friendly fluidic interconnection and alignment-free piezoelectric readout by using laser-pulled glass capillary and QTF without relying on any conventional microfabrication process. After the proposed system is constructed and thoroughly characterized, it is successfully applied to precision density measurements for various liquid samples and size characterization of microscale oil droplets suspended in water.

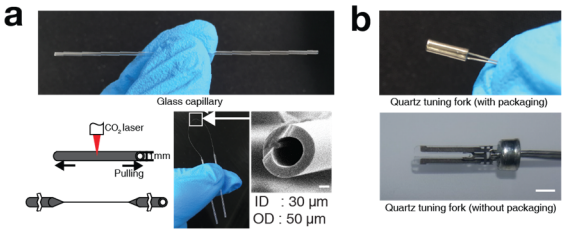

Figure 1: Glass capillary and quartz tuning fork (QTF) components for configuring the pulled microcapillary tube resonator (PμTR). (a) A glass capillary (top). Schematic showing the capillary pulling to decrease the inner and outer diameters around the middle section of the capillary (bottom left). A pulled capillary (bottom middle) with scanning electron micrographs of cross-section areas of pulled capillary. Scale bar is 10 μm (bottom right). (b) A QTF before (top) and after (bottom) the package is opened and removed. The scale bar is 1 mm.

FABRICATION

To fabricate the PμTR, we employ a laser-pulling process to a borosilicate glass capillary of which inner and outer diameters are 0.58 and 1.00 mm, respectively, (Fig. 1a) (1B100F-3, World Precision Instruments.) using a commercial pipette puller (P-2000, Sutter Instruments). The laser heated pipette puller defines the microcapillary tube through sequential heating and pulling processes which locally stretch the middle section of the glass capillary while maintaining the cross-sectional area of both ends. Inner and outer diameters of the pulled section of the glass microcapillary can be varied by adjusting parameters such as laser power, pulling force and distance. We fabricate the microcapillary of which inner and outer diameters are 30 and 50 μm and overall elongation length is 58 mm.

For sensing of the resonance frequency of fabricated microcapillary, a commercial QTF (AB26T-32.768 kHz, Abracon) is employed after its hermetic metal can packaging is removed (Fig. 1b). For actuation the microcapillary, a piezo actuator (TA0505D024W, Thorlabs) is employed. Figure 1c illustrates the overall schematic of the PμTR. A microcapillary tube contacts with a solid block on top of a piezo actuator and one prong

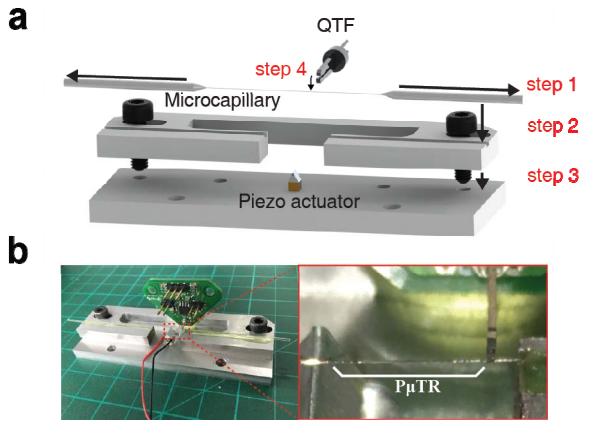

Figure 2: Assembly process of PμTR platform. (a) Assembly process of PμTR system (not to scale). (b) Photographs of an assembled PμTR sensing platform ready for testing.

of a QTF. The contact point above the piezo actuator becomes the actuation node while the contact point with the QTF becomes the sensing node. The node-to-node distance (i.e. distance between two contact points) defines the length of the PμTR. Unpulled sections at both ends facilitate interfacing with standard fluidic components.

To realize the proposed PμTR, parts are assembled by following the procedures in Fig. 2a. First, 0.3 N of axial tension is applied to a pulled microcapillary using a tension gauge (110g, OHBA SIKI) to remove slacks and also increase the resonance frequency of PμTR (step 1). With the applied tension maintained, the pulled microcapillary is brought over and attached to a custom machined aluminum jig with an epoxy bonding (step 2). Then, the jig holding the attached microcapillary is fixed to a base block having a nodal block on the piezo actuator with two standard M4 bolts (step 3). After this step, the pulled microcapillary make a solid contact with the actuation node. Finally, using a motorized stage (MTS25-Z8, Thorlabs), the QTF mounted on a custom printed circuit board (PCB) approaches precisely with a 10-μm step towards the pulled microcapillary and make another solid contact which defined the sensing node (step 4). The PCB is bonded to the jig assembly by using the epoxy. Figure 2b shows pictures of the final PμTR system. The node-to-node resonance distance was set to 6.5 mm.

VALIDATION

The resonance frequency f, of the PμTR under axial tension T, is given by

$$f = \frac{1}{2d}\sqrt{\frac{T}{m_d} + \left(\frac{\pi}{d}\right)^2 \frac{EI}{m_d}} \qquad (1)$$

where d is the PμTR's length, E is the Young's modulus, I is the area moment of inertia, and m_d is the mass per unit length of the PμTR, respectively. When the operation of the actuating node induces out-of-plane vibration of the PμTR, the vertical reflection force, F_v, which is the vertical component of the applied axial tension, is felt by the QTF and is given by

$$F_v = T\sin\theta \cong T\theta \propto TA(2\pi f_E t + \phi) \qquad (2)$$

where θ is the tangent angle of the PμTR at the QTF sensing node, A is the vibration amplitude, f_E is the

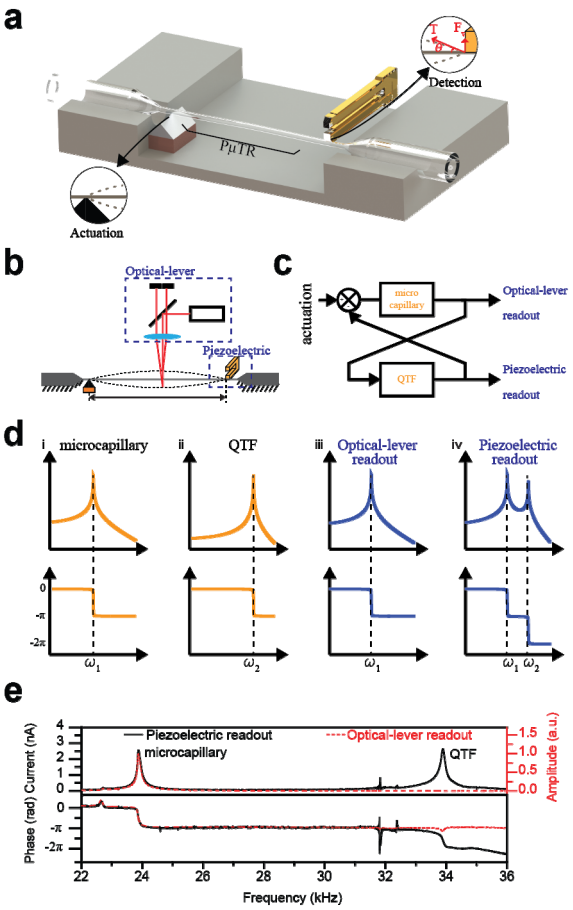

Figure 3: Operation of the PμTR and signal transfer analysis. (a) Actuating and sensing schematics of PμTR. (b) Experimental schematic for additional optical-lever readout. (c) Block diagram for the PμTR system. (d) Amplitude and phase spectra of individual components and combined PμTR system obtained by optical-lever and piezoelectric readouts. (e) Amplitude and phase spectra of a water-filled PμTR measured by the two readout schemes.

excitation frequency, t is time, and ϕ is the phase delay (Fig. 3a). This vertical reflection, F_v, of which magnitude is proportional to the vibration amplitude of the PμTR is transmitted to the QTF, then, induces a forced vibration at one of two prongs with the frequency of f_E. Dynamic force applied to the QTF prong by an external input of F_v is transduced to electrical current due to the intrinsic piezoelectric effect of QTF. For amplifying and current to voltage converting, a transimpedance amplifier (OPA129, Texas Instruments) is configured with a 200 kΩ gain resistor and connected to one electrode of the QTF while the other electrode of QTF is grounded.

The proposed operation scheme of PμTR using QTF readout somewhat different from the general MEMS resonator detection schemes, thus we validate it by comparing with the conventional optical-lever detection, typically used for atomic force microscopy. To this end, a custom optical-lever setup is built with a laser diode, a beam splitter, a focusing lens, and a two-segmented photodiode as shown in Fig. 3b. For two readout schemes, signal transfers in the PμTR can be understood by the block

diagram (Fig. 3c). Once an external excitation signal vibrates the microcapillary, the vibration of the microcapillary is transmitted to the QTF and the response by the QTF reflects back to the microcapillary. Since the QTF prong is a second order mechanical system, responses at frequency higher than the QTF resonance will be attenuated. To avoid this, we design the resonance frequency of the microcapillary lower than the resonance frequency of QTF (Figs. 3d(i) and d(ii)). With this arrangement, the optical-lever readout only shows the resonance of the microcapillary (Fig. 3c(iii)). In contrast, the piezoelectric readout captures two resonance behaviors, one for the microcapillary and the other for the QTF itself (Fig. 3c(iv)).

Figure 3e shows amplitude and phase spectra from the two readouts by using open-loop frequency sweep mode with a lock-in amplifier (Model 7265, Signal Recovery). While the piezoelectric readout captures two resonance peaks, one near 24.5 kHz for PμTR and the other near 33.0 kHz for QTF, the optical-lever readout measures a single resonance peak at 24.5 kHz for PμTR. These frequency responses agree well with the simulated resonance spectra and prove the simple piezoelectric readout scheme by using QTF can measure the resonance frequency of the PμTR.

After operation schematic validation, mass responsivity of PμTR is calibrated by resonance shift measurement with various liquid filling inside the microcapillary. Water and ethanol are sequentially introduced into the PμTR (Fig. 4a). Then, for more precise calibration, various ethanol-water and glycerol-water binary mixtures are prepared and injected in the PμTR while the resonance frequency of PμTR is measured (Fig. 4b). From the linear regression of the frequency shift vs. density plot, the density responsivity of –3,088 Hz-g^{-1}cm^3 is extracted at room temperature.

MICRO DROPLET SIZE MEASUREMENT

A microscale droplet generator is configured at one entrance of the PμTR as shown in Fig. 5a. Mineral oil is used as a disperse phase and water is used as a continuous phase (i.e. mineral oil droplets in water). In the water, a surfactant (Tween20, Sigma Aldrich) is mixed at a volume fraction of 0.5 percent. When micro scale oil droplets generated enter the pulled section of the PμTR, they are squeezed and become plugs since their diameters are larger than the inner diameter of the pulled section as shown in Fig. 5b (top). Once they come out of the pulled section of the PμTR, their shapes are restored back to spheres and

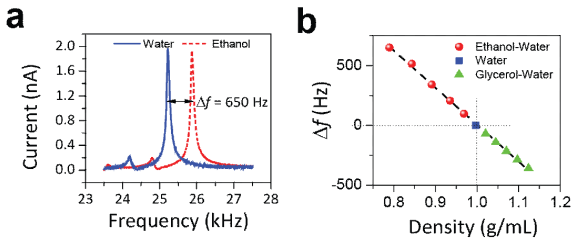

Figure 4: Liquid density measurements and responsivity calibration. (a) Resonant spectra of a 6.5-mm long PμTR filled with water and ethanol. (b) The liquid density responsivity of –3,088 Hz-g^{-1}cm^3 is obtained from the linear regression.

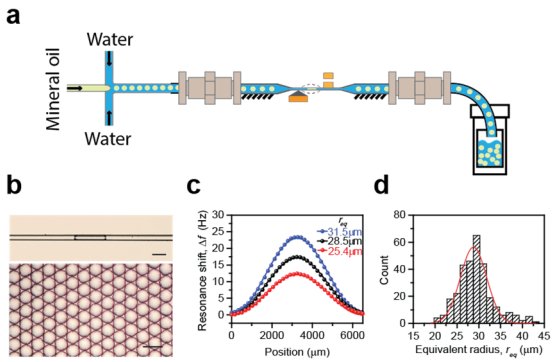

Figure 5: Oil micro droplets size measurement. (a) A micro droplet generator configured at the inlet of the PμTR for real-time monitoring of droplet size. (b) Optical micrographs of a squeezed oil plug passing through the PμTR (top) and collected spherical droplets after measurements (bottom). Scale bars in both images are 100 μm. (c) Resonance frequency shifts fitting upon a transit of mineral oil plugs of which equivalent radii are 25.4, 28.5 and 31.5 μm, respectively. (d) Histogram for the equivalent radius of oil droplets.

collected in the outlet vial (Fig. 5b (bottom)). During the oil droplet sizing, the PμTR is operated in the closed-loop feedback mode while its resonance frequency is down-mixed to ~1 kHz with a reference sine wave from a function generator (33220A, Agilent) and then measured with a 100 MHz frequency counter in the data acquisition board (USB6361, National Instruments).

Since the length of squeezed oil plugs are in general much shorter than the node-to-node distance, the assumption of a point mass traveling through the long string resonator is valid. Figure 5c shows resonance frequency shifts of the PμTR recorded when oil plugs with three different lengths passed through the PμTR. To quantify equivalent radii of oil plugs, buoyant mass of each plug is first calculated from fitting measured resonance shift data with the theoretical estimations given by [8]

$$\frac{\Delta f}{f_w} = \frac{1}{\sqrt{1+2\frac{m_{op}}{m_r}\sin^2(\frac{\pi x}{d})}} \tag{3}$$

where Δf is the resonance frequency shift due to an oil plug transiting the PμTR, f_w is the resonance frequency of the PμTR entirely filled with water, m_{op} is the buoyant mass of the oil plug, m_r is the mass of the PμTR, and x is the lateral position of the traveling oil plug. After measuring the mass of oil plug, its equivalent spherical radius, r_{eq}, can be given by

$$r_{eq} = \left(\frac{3}{4\pi}\frac{m_{op}}{\rho_w - \rho_o}\right)^{1/3} \tag{4}$$

where ρ_w and ρ_o are densities of water and mineral oil, respectively. A histogram of the equivalent oil micro droplet radius is acquired with the average of 28.47 μm and the standard deviation of 4.03 μm (Fig. 5d).

The detection resolution of the difference in equivalent radii of oil plugs ($\Delta r_{eq} \equiv \sigma_A/R_r$) is obtained by dividing the Allan deviation (σ_A) of the PμTR from the radius responsivity ($R_r = \frac{df}{dr}$). The chain rule is applied to the radius responsivity to include the buoyant mass of oil plugs (m_{op}) as follows.

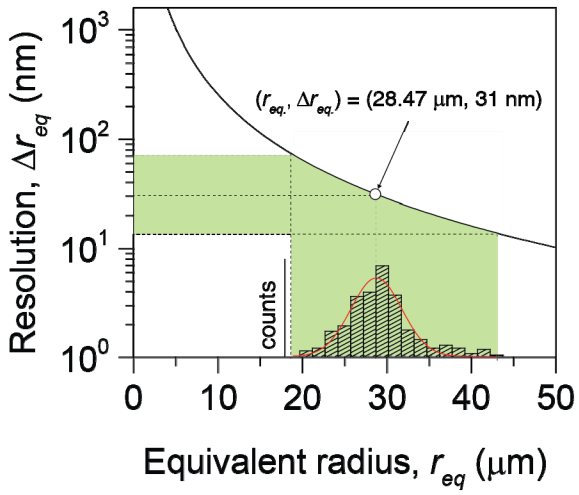

Figure 6: Detection resolution of the difference in oil droplet radius as a function of the equivalent oil droplet radius (calculated from frequency stabilities, $1\sigma_A$). Figure 5d is included as inset histogram plot to show the radius distribution of measured oil plugs.

$$\Delta r_{eq} = \frac{\sigma_A}{\frac{df}{dr}} = \frac{\sigma_A}{\frac{df}{dm_{op}}\frac{dm_{op}}{dr}} \quad (5)$$

The derivative of $\frac{dm_{op}}{dr}$ derived by spherical mass-volume relationship ($m_{op} = 4\pi/3 \cdot r^3(\rho_w - \rho_o)$) is given by

$$\frac{dm_{op}}{dr} = 4\pi r^2(\rho_w - \rho_o) \quad (6)$$

Then, by employing Equation (6) to Equation (5), the relationship between the mass and radius resolutions is obtained as

$$\Delta r_{eq} = \frac{\Delta m}{4\pi r^2(\rho_w - \rho_o)}, \ \Delta m \equiv \frac{\sigma_A}{R_m} \quad (7)$$

The mass responsivity ($R_m = \frac{df}{dm}$) is acquired by fitting data of transiting oil plugs shown in Figs. 5c and 5d. Equation (7) indicates that the radius resolution is inversely proportional to the square of its own radius.

Figure 6 shows the detection resolution of the difference in mineral oil droplet radius, Δr_{eq}, plotted as a function of the equivalent oil droplet radius. This resolution is calculated from frequency stabilities, 1 σ_A. For the average droplet radius of 28.47 μm, PμTR system can differentiate oil droplets if their radius differ by approximately 31.66 nm based on the 1 σ_A criteria. As the droplet gets smaller, the resolution of Δr_{eq} becomes negatively affected.

CONCLUSION

Here, we propose a microfabrication-free approach to realize microscale fluidic resonators for droplet size measuring applications by simple laser pulling method and configuring three off-the-shelf parts; glass capillary, piezo actuator, and quartz tuning fork. The PμTR system also offers the align-free piezoelectric readout of the resonance frequency and facile connection to standard tubings and fluidic components. And the PμTR system shows more precise and quantitative measurements for droplet sizing than general optical microscopy. We expect that the developed PμTR would be useful for characterization and monitoring applications of microscale droplets and particles.

ACKNOWLEDGEMENTS

This research was supported by the Commercialization Promotion Agency for R&D Outcomes (COMPA) (2015K000127) and the National Research Foundation of Korea (NRF) funded by the Korea government (MSIP) (NRF-2015K1A3A1A21000288 and NRF-2013R1A1A1076080).

REFERENCES

[1] R. A. Barton, B. Ilic, S. S. Verbridge, B. R. Cipriany, J. M. Parpia, H. G. Craighead, "Fabrication of a nanomechanical mass sensor containing a nanofluidic channel", *Nano Lett.,* vol. 10, pp. 2058-2063, 2010.

[2] M. F. Khan, S. Schmid, Z. J. Davis, S. Dohn, A. Boisen, "Fabrication of resonant micro cantilevers with integrated transparent fluidic channel", *Microelec. Eng.,* vol. 88, pp. 2300–2303, 2011.

[3] T. P. Burg, M. Godin, S. M. Knudsen, W. Shen, G. Carlson, J. S. Foster, K. Babcock, S. R. Manalis, "Weighing of biomolecules, single cells and single nanoparticles in fluid", *Nature,* vol. 446, pp. 1066–1069, 2007.

[4] J. Lee, W. Shen, K. Payer, T. P. Burg, S. R. Manalis, "Toward attogram mass measurements in solution with suspended nanochannel resonators", *Nano Lett.* vol. 10, pp. 2537–2542, 2010.

[5] J. Kim, J. Song, K. Kim, S. Kim, J. Song, N. Kim, M. F. Khan, L. Zhang, J. E. Sader, K. Park, D. Kim, T. Thundat, J. Lee, "Hollow microtube resonators via silicon self-assembly toward subattogram mass sensing applications", *Nano. Lett.*, vol. 16, pp. 1537–1545, 2016.

[6] O. Malvar, D. Ramos, C. Martinez, P. Kosaka, J. Tamayo, M. Calleja, "Highly sensitive measurement of liquid density in air using suspended microcapillary resonators", *Sensors*, vol. 15, pp. 7650–7657, 2015.

[7] M. Mauro, R. Battaglia, G. Ferrini, R. Puglish, D. Balduzzi, A. Galli, "Experimental evidence of a buoyant mass difference between bovine spermatozoa bearing X- and Y-chromosomes using a micromechanical resonator", *Analyst*, vol. 139, pp. 1148–1154, 2014.

[8] S. Schmid, S. Dohn, A. Boisen, "Real-time particle mass spectrometry based on resonant micro strings", *Sensors*, vol. 10, pp. 8092–8100, 2010.

CONTACT

*Jungchul Lee, tel: +82-2-705-7973,
jayclee@sogang.ac.kr